Environmental vibrations and noise due to offshore installation of foundation piles

Apostolos Tsouvalas [i)], Yaxi Peng [ii)], Timo Molenkamp [iii)] and Ozkan Sertlek [iv)]

i) Assistant Professor, Faculty of Civil Engineering and Geosciences, Department of Engineering Structures, Delft University of Technology, Stevinweg 1, 2628CN Delft, The Netherlands.

ii) Ph.D. candidate, Faculty of Civil Engineering and Geosciences, Department of Engineering Structures, Delft University of Technology, Stevinweg 1, 2628CN Delft, The Netherlands.

ii) Ph.D. candidate, Faculty of Civil Engineering and Geosciences, Department of Hydraulic Engineering, Delft University of Technology, Stevinweg 1, 2628CN Delft, The Netherlands.

iv) Postdoctoral researcher, Faculty of Civil Engineering and Geosciences, Department of Hydraulic Engineering, Delft University of Technology, Stevinweg 1, 2628CN Delft, The Netherlands.

ABSTRACT

Foundation piles are often used to support offshore structures such as oil and gas platforms or offshore wind power generators. The pile installation process, which is a key step in the construction of many structures offshore, is hindered by a serious by-product; seabed vibrations and underwater noise pollution. Seabed vibrations and noise have drawn the attention of many environmental organisations and regulatory bodies worldwide. In particular, the noise emission is strictly regulated nowadays, especially when it comes to impact piling noise. When noise levels exceed the thresholds set by the (inter)national authorities, noise mitigation is often required. This paper reviews the state-of-the-art computational methods to predict the underwater noise emission and the associated seabed vibrations by the installation of foundation piles offshore. Various noise mitigation strategies are discussed and the modelling framework applied to predict noise mitigation in the case of air-bubble curtains is presented in more detail. A brief overview of the available noise regulations in Europe and abroad is also given. The paper identifies the future challenges in the field under the prism of the ever-increasing size of piles and the new pile driving technologies.

Keywords: offshore piles, underwater noise, seabed vibrations, impact hammer, noise regulations, offshore wind.

1 INTRODUCTION

Driven by the ambitious climate goals to reduce greenhouse gas emissions, the demand for energy generated by wind turbines increased in the past decades (Perveen et al. , 2014; Fried et al., 2017). To support the wind turbines, several foundation concepts exist such as monopiles, tripods, steel jackets, suction caissons and gravity-based foundations (Oh et al.. 2018; Wu et al., 2019). The choice of the most appropriate concept is governed by several factors like the water depth, the seabed conditions, the expected sea wave heights and the presence of currents (Lozano-Minguez et al., 2011). Despite the plethora of available foundation types, the monopile is the most common foundation type for wind turbines installed at shallow waters (EWEA, 2019).

Monopiles are driven into the seabed with either hydraulic impact hammers or large vibratory devices (Thomsen, 2012). In impact piling, the hammer delivers a series of short duration pulses at the pile head which drive the pile into the sediment. In contrast, when vibratory techniques are used, the pile is forced gradually into the soil by introducing a periodic excitations at the pile head (Warrington, 1989). Regardless of the installation method chosen, noise is generated in the seawater and elastic waves radiate into the seabed. The characteristics of the radiated wave field relate strongly to the method of installation, the pile size and the local site conditions (Tsouvalas, 2015). These elements are key to understand the noise pollution and the uncertainty in the propagation of the sound field at large distances (Farcas et al., 2016).

Next to the modelling efforts to quantify the noise levels in the seawater, many studies focus on the impact of anthropogenic noise emissions on the aquatic species (Popper and Hastings, 2009; Finneran, 2015]. In impact piling, each strike of the hydraulic hammer generates strong impulsive sound waves in the seawater which propagate at large distance from the pile (Bailey et al., 2010). The responses of marine mammals and fish to the noise ranges from light disturbance to strong avoidance of the construction site; in extreme cases yielding even permanent hearing impairment (Herbert-Read et al., 2017; Hastie et al., 2019). The extent of auditory damage depends on the frequency content of the radiated sound, the duration of exposure to high noise levels and the auditory characteristics of the species (Kastelein et al., 2013). The underwater sound emission when piles are installed with vibratory devices is less thoroughly explored. However, a few studies do exist which try to quantify the noise levels (Tsouvalas and Metrikine, 2016) and assess the environmental impact (Graham et al., 2017). Even scarcer are studies which investigate systematically the behavioural response of marine mammals when noise mitigation systems are employed (Dähne et al., 2017).

The high noise levels generated by offshore construction activities have drawn the attention of regulatory authorities in several nations (Erbe, 2013). The German Federal government sets specific requirements on the maximum sound levels allowed: 160 dB for the sound exposure level and 190 dB for the sound peak pressure level. Both values are being measured at 750 m from the pile and referenced to 1 μPa (Lucke et al., 2009). In The Netherlands, regulations adopt specific sound level criteria (Ainslie, 2011; De Jong et al., 2011). The latter are similar to those imposed in Germany, but consider additionally cumulative noise exposure levels. In the United Kingdom, an environmental impact assessment (EIA) is followed per project in which acoustic deterrent devices (seal scarers) are used (Brandt et al., 2013) together with trained marine mammal observers who monitor the activity on site (Dolman and Simmonds, 2010). The majority of the regulations do not consider in detail the frequency content of the radiated noise; an item worth investigating in the near future (Stöber and Thomsen, 2019).

This paper presents the state-of-the-art computational methods to prognosticate the underwater sound during offshore pile installation including the available methods to mitigate the noise. Section 2 covers the state-of-the-art in modelling noise due to impact piling. Section 3 presents results of numerical computations for some realistic cases in order to illustrate the importance of some key features for the control of the noise and vibration paths. In Section 4, noise mitigation techniques and modelling are discussed. Section 5 describes a few key challenges under the prism of future developments in the field. Section 6, gives an overview of the regulations in Europe and abroad distinguishing between impulsive and non-impulsive noise fields. Finally, Section 7 concludes with an overview of the content of the paper.

2 THE STATE-OF-THE-ART IN MODELLING SOUND EMISSION AND SEABED VIBRATIONS

Acoustic models can be categorised into several groups based on the degree of detail in modelling the sound source and/or the domain in which the energy is released. Given this categorisation, models can span a whole range from empirical ones to very detailed numerical ones. Section 2.1 discusses the state-of-the-art empirical models to estimate sound levels in the case of impact piling. Section 2.2 presents the mathematical statement of the coupled pile-water-soil system while sections 2.3 discusses the semi-analytical and the numerical approaches which are employed to solve the mathematical statement of the problem. Section 2.4 concludes with a concise overview of all models available to date.

2.1 Empirical models

In empirical models, the acoustic source is described as a sound level at a reference location. Subsequently, this reference sound level is propagated at larger distances by means of a transmission loss formula which is based on the source–receiver distance and the characteristics of the acoustic domain under consideration (Mercer, 1962). Attempts to apply similar methods in impact piling and vibratory installation have also been reported (Lippert et al., 2018; Martin and Barclay, 2019). The most recent formula proposed to estimate the (averaged over the depth of the water column) sound exposure level $\mathrm{L_E}$ from impact piling reads:

$$L_E(r) = L_E(r_1) - 10\log_{10}\left(\frac{r}{r_1}\right) - \alpha(r - r_1) \tag{1}$$

In Equation (1), r is the radial distance from the pile, r_1 defines the reference range in which the sound level is k nown and α is a frequency-independent decay factor in dB m^{-1}:

$$\alpha = -\frac{10\log_{10}(|R|^2)}{2\mathrm{H}\coth(\theta)} \tag{2}$$

The loss at bottom interaction is described in terms of the squared magnitude of the reflection factor R between water and assumed seabed half-space, the angle q represents the angle of Mach cone (about 17°) and H is the water depth in meters. The depth-averaged sound exposure level $\mathrm{L_E}$ at the reference range $\mathrm{r_1}$ can be derived on the basis of measurements:

$$L_E = 10\log_{10}\left(\frac{1}{\mathrm{p}_0^2 T_0}\int_{t=t_1}^{t=t_2} p^2(t)dt\right) \tag{3}$$

in which $T_0 = 1$ s, $p_0 = 10^6$ Pa, and the impulsive si gnal being fully enclosed between the time moments $\mathrm{t_1}$ and $\mathrm{t_2}$. The physical quantity p^2(t) corresponds to depth -averaged squared sound pressure from the signal alone, excluding all other sources of acoustic noise. The DCS model proposed by Lippert et al. (2018) has been adjust ed recently for environments of varying bathymetry and seabed properties by Martin and Barclay (2019).

For the estimation of the peak pressure level $\mathrm{SPL_{peak}}$ a similar formula is proposed that requires as input the $\mathrm{L_E}$ and the properties of the hammer strike (Lippert et al ., 2015):

$$\mathrm{SPL_{peak}} = \mathrm{A\ L_E} + \mathrm{B} + \mathrm{C}\ (\left[\frac{\mathrm{Z_p}}{\mathrm{m_r}}\right]_0 - \left[\frac{\mathrm{Z_p}}{\mathrm{m_r}}\right]_1) \tag{4}$$

The subscript indices in the squared brackets stand for the site from which the regression coefficients A and B are derived (0) and the unknown site for which the $\mathrm{SPL_{peak}}$ is to be estimated (1), with the empirical factor C having the unit [dB s]. Additionally, m_r is the mass of the hammer and $Z_p = E_p A_p / c_p$ is the pile impedance, with E_p being the Young's modulus of the pile, A_p its cross-sectional area and cp the axial wave velocity in the pile.

Equations (1)-(4) are useful for a quick prognosis of the noise levels at a given location, especially when the values of the decay factor α in Equation (1) can be estimated with reasonable accuracy. However, their use should be exercised with caution and only when one fully understands their inherent limitations. First, one should be able to obtain the sound level in the pile proximity which can then be inserted into an empirical model for sound transmission. Second, one should feel confident that the estimation of the decay factor α at the location of interest is reasonable. Third, the formulae can only be used to estimate the sound exposure level $\mathrm{L_E}$, and possibly the $\mathrm{SPL_{peak}}$ with some degree of confidence; a complete picture of the sound field cannot be retrieved in this case.

2.2 The mathematical statement of the linear pile-soil-water interaction problem

Most advanced models treat the problem in two steps as illustrated in Figure 1. A close-range module is used to generate the wave field at pile proximity ($r \leq r_0$) and this field is subsequently coupled at $r = r_0$ to a far-range module for the propagation of sound at larger distances ($r = r_0$). The basic model is cylindrically symmetric and consists of the pile and the surrounding media, i.e., the seawater domain overlying a stack of horizontally stratified elastic layers. Let us assume that the pile is of finite length and occupies the domain $0 \leq z \leq L$. The constants R, t, ν and ρ define the radius, thickness, Poisson's ratio and density of the shell, respectively. The fluid is modelled as a three-dimensional inviscid compressible medium having a pressure release boundary at $z = z_0$ and occupying the domain $z_0 \leq z \leq z_1$, $r \geq R + t/2$. The seabed is modelled as a three-dimensional elastic continuum which occupies the domain $z_1 \leq z < \infty$, $r \geq R + \frac{t}{2}$. The constants λ_{s_j}, μ_{s_j} and ρ_{s_j} define the *Lamê* coefficients and the density of each solid layer, respectively.

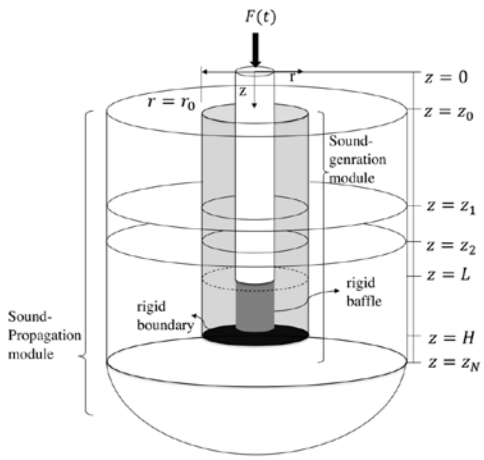

Fig. 1. Schematic of the coupled model: r_0 is the radial distance of the coupled cylindrical surface marking the boundary between the near- and far-field models; z_0 is the level of the sea surface; z_1 is the level of the seabed; z_j is the bottom level of the j-th soil layer ($j = 2,3 \ldots N$). The impact hammer or vibratory device is substituted by an external force at the pile head.

The dynamics of the total system are described by the following set of partial differential equations:

$$\mathbf{L}\tilde{\mathbf{u}}_p + \tilde{\mathbf{I}}\tilde{\mathbf{u}}_p = \big(H(z - z_1) - H(z - L)\big)\tilde{\mathbf{t}}_s - \big(H(z - z_0) - H(z - z_1)\big)\tilde{\mathbf{P}}_e + \tilde{\mathbf{f}}_e \tag{5}$$

$$\mu_s \nabla^2 \tilde{\mathbf{u}}_s + (\lambda_s + 2\mu_s)\nabla\nabla \cdot \tilde{\mathbf{u}}_s = \omega^2 \rho_s \tilde{\mathbf{u}}_s \tag{6}$$

$$\nabla^2 \tilde{\phi}_f(r, z, \omega) + \frac{\omega^2}{c_f^2}\tilde{\phi}_f(r, z, \omega) = 0 \tag{7}$$

In Equations (5)-(7), $\tilde{\mathbf{u}}_p = \left[\tilde{u}_{p,z}(z,\omega), \tilde{u}_{p,r}(z,\omega)\right]^T$ is the displacement vector of the mid-surface of the shell, $\tilde{\mathbf{u}}_s = \left[\tilde{u}_{s,z}(z,\omega), \tilde{u}_{s,r}(z,\omega)\right]^T$ is the displacement vector of each solid layer. The function $\tilde{\phi}_f(r, z, \omega)$ is a displacement potential introduced for the description of the fluid with c_f being the speed of the compressional wave speed. The operators $\mathbf{L}$ and $\tilde{\mathbf{I}}$ are the stiffness and modified inertia matrices of the shell, respectively (Tsouvalas, 2015). The term $\tilde{\mathbf{P}}_e$ represents the fluid pressure exerted at the outer surface of the shell at $z_0 < z < z_1$. The functions $H(z - z_i)$ are Heaviside step functions, which are used here to account for the fact that the soil and the fluid are in contact with different segments of the shell. The vector $\tilde{\mathbf{f}}_e = \left[\tilde{f}_{rz}(z,\omega), \tilde{f}_{rr}(z,\omega)\right]^T$ represents the externally applied force on the surface of the shell. The term $\tilde{\mathbf{t}}_s$ represents the boundary stress vector that takes into account the reaction of the soil surrounding the shell at $z_1 < z < L$. At the soil-water interface, the vertical stress equilibrium and the vertical displacement continuity are imposed, whereas the shear stress at the surface of the upper solid layer vanishes. A set of boundary conditions and interface conditions are formulated as follows and are satisfied at $r \geq R$:

$$\tilde{p}_f|_{z=0} = 0 \tag{8}$$

$$\frac{\tilde{v}_{f,z}}{i\omega} = \tilde{u}_{s,z}|_{z=z_1}, \quad \tilde{p}_f = -\tilde{\sigma}_{zz}^{-}|_{z=0}, \quad \tilde{\sigma}_{zr}|_{z=0} \tag{9}$$

$$\tilde{u}_{s,z}^{+} = \tilde{u}_{s,z}^{-}|_{z=D_j}, \quad \tilde{u}_{s,r}^{+} = \tilde{u}_{s,r}^{-}|_{z=D_j}, \quad \tilde{\sigma}_{zz}^{+} = \tilde{\sigma}_{zz}^{-}|_{z=D_j}, \quad \tilde{\sigma}_{zr}^{+} = \tilde{\sigma}_{zr}^{-}|_{z=D_j} \tag{10}$$

$$\tilde{u}_{s,z}|_{z=H} = 0, \quad \tilde{u}_{s,r}|_{z=H} = 0 \quad \text{for } r \le r_0 \tag{11}$$

In addition to Equations (8)-(11), the radiation condition needs to be satisfied at $r \to \infty$. In the far-from-source module, the lower boundary conditions at $z = H$ are substituted by the radiation condition at $z \to \infty$.

It is important to realize that the mathematical statement of the problem given by the system of coupled partial differential equations (PDEs) (5)–(11) is similar in all available models with only some minor modifications in the boundary/interface conditions or in approximations made for the far-range model. This is despite the fact that the solution approach may differ significantly between the various methods. Numerical methods employ either finite elements or finite differences to reduce the system of coupled PDEs to a system of Ordinary Differential Equations (ODEs) by means of direct spatial discretization. Semi-analytical methods usually transform the set of Equations (5)–(11) into the frequency domain first and proceed further with the solution as discussed in the sequel.

2.3 Solution methods

The solution to the system of mathematical equations (5)-(11) can be obtained by applying either semi-analytical or numerical techniques. Semi-analytical models can vary significantly in complexity based on different underlying assumptions. Hereafter, the model introduced in (Peng et al., 2021a) is discussed further. The dynamic responses of the shell structure and the acousto-elastic waveguide (in the frequency domain) are expressed in terms of free vibration modes. The modal expansion of the shell structure reads:

$$\tilde{u}_{p,k}(z,\omega) = \sum_{m=1}^{\infty} A_m U_{km}(z) \tag{12}$$

The index $k = z, r$ indicates the displacement component, $m = 1, 2, \dots, \infty$ is the axial order and the vertical eigenfunctions $U_{km}(z)$ satisfy the boundary conditions at z = 0, L. The closed form expressions for the acousto-elastic field, which satisfy the boundary conditions including the radiation condition at $r \to \infty$, read:

$$\tilde{p}_f(r,z,\omega) = \sum_{p=1}^{\infty} C_p H_0^{(2)}\left(k_r^{(p)} r\right) \tilde{p}_{f,p}(z) \tag{13}$$

The expressions for the displacement and stress field are presented in similar form in (Tsouvalas, 2015) and are omitted here for the sake of brevity. In Equations (12)–(13), the only unknowns are the modal coefficients A_m and C_p which can be determined by solving the forced response of the complete system:

$$\sum_{p=1}^{\infty} C_p \left(L_{qp} + k_r^{(q)} H_1^{(2)}\left(k_r^{(q)} R\right) \gamma_q \delta_{qp} - \sum_{m=1}^{\infty} \frac{R_{mq} Q_{mp}}{I_m} \right) = \sum_{m=1}^{\infty} \frac{F_m Q_{mp}}{I_m} \tag{14}$$

$$A_m = \frac{F_m + \sum_{p=1}^{\infty} C_p R_{mp}}{I_m} \tag{15}$$

A detailed derivation of the terms L_{qp}, γ_q , Q_{mp}, R_{mq} and I_m introduced in Eqs. 3 is given in (Tsouvalas and Metrikine, 2014). By following the approach above, the original system of PDEs is reduced to an infinite system of algebraic equations, i.e., Equation (14), provided that the modal expansions over the shell and acousto-elastic modes are properly truncated.

Once the near-source wave field is computed up to a distance r_0, it can be coupled to a propagation algorithm to compute the response at $r > r_0$. There are several ways to achieve this as described in detail in (Tsouvalas, 2020). By utilizing Betti's reciprocal theorem in elastodynamics and Green's theorem for acoustic problem, the complete solution for the acousto-elastic domain can be obtained by evaluating the following boundary integral:

$$\tilde{u}_\alpha^{\Xi}(\boldsymbol{r},\omega) = \sum_{\beta = r,z} \int_{S^s} (\tilde{U}_{\alpha\beta}^{\Xi s}(\boldsymbol{r},\boldsymbol{r_0},\omega) \cdot \tilde{t}_\beta^n(\boldsymbol{r_0},\omega) - \tilde{T}_{\alpha\beta}^{n,\Xi s}(\boldsymbol{r},\boldsymbol{r_0},\omega) \cdot \tilde{u}_\beta(\boldsymbol{r_0},\omega)) dS^s(\boldsymbol{r}_0) + \int_{S^f} (\tilde{U}_{\alpha r}^{\Xi f}(\boldsymbol{r},\boldsymbol{r_0},\omega) \cdot \tilde{p}\,(\boldsymbol{r_0},\omega) - \tilde{T}_{\alpha r}^{n,\Xi f}(\boldsymbol{r},\boldsymbol{r_0},\omega) \cdot \tilde{u}_r(\boldsymbol{r_0},\omega))\, dS^f(\boldsymbol{r}_0), \boldsymbol{r} \in V \tag{16}$$

in which n is the outward normal to the cylindrical boun dary. The superscripts of the Green's tensors, "f" and "s" indicate fluid and soil domains, respectively. By kn owing $\tilde{t}_\beta^n(\boldsymbol{r_0},\omega)$, $\tilde{u}_\beta(\boldsymbol{r_0},\omega)$, $\tilde{p}\,(\boldsymbol{r_0},\omega)$, and $\tilde{u}_r(\boldsymbol{r_0},\omega)$ at a given cylindrical boundary r_0, Equation (16) can be app lied to propagate the field at any position $r > r_0$.

Finite element packages or finite difference schemes can also be employed to solve the mathematical stateme nt given by Equations (5) - (11). These spatial discretiza tion methods (FEM or FDM) are primarily used to gene rate the acoustic field in the pile proximity while a soun d propagation model is used to compute the field at larg er distances from the pile. A comprehensive overview o f the numerical models is given in (Lippert et al., 2016).

2.4 Overview of noise prediction models

Table 1 provides a list of all available models which have been validated either against experimental data or numerical benchmark studies.

Table 1. List of existing models to predict noise by impact piling.

Model	Modelling Approach	Remarks
CMST	***Close-range:*** PACSYS (2020) ***Long-range:*** ORCA (Westwood et al., 1996)	– Axisymmetric model. – Seabed modelled as fluid. – Extension to full 3D possible in the long-range module.
TUHH	***Close-range:*** ABAQUS (Heitmann et al., 2015) ***Long-range:*** WI algorithm (Von Pein et al., 2019)	– Axisymmetric model. – Close-range module includes elasticity of the seabed. – Range- and angular-dependent environments can be included within the all-fluid model approximation in the long-range module.
JASCO	***Close-range:*** FDTD (MacGillivray, 2015) ***Long-range:*** WI algorithm	– Axisymmetric model. – Seabed modelled as fluid. – Simplification of the shell theory with no bending energy stored in the shell surface.
SNU	***Close-range:*** FE model (Park et al., 2013) ***Long-range:*** PE model (Collins, 1993)	– Axisymmetric model. – Seabed modelled as fluid. – Range- and angular-dependent environments can be included within the all-fluid model approximation in the long-range module.
UoS/NPL	***Close-range:*** FE model ***Long-range:*** BE model (Wood, 2016)	– Axisymmetric model. – Seabed modelled as fluid.
AQUARIUS (TNO)	***Close-range:*** FE model (Zampolli et al., 2013) ***Long-range:*** NM model (Zampolli et al., 2013)	– Axisymmetric model. – 3D effects in terms of range-dependent environments through the adoption of adiabatic theory for the normal modes within the all-fluid
SILENCE (TUD)	***Close-range:*** Semi-analytical model (Tsouvalas, 2015) ***Long-range:*** Boundary element (BE) model (Peng et al. 2021a)	– Axisymmetric model including a layered elastic seabed description at both close- and long-range modules. – Range-dependency with the all-fluid approximation in the long-range module (Sertlek et al., 2019; Sertlek and Ainslie, 2014). – Modelling of the air bubble curtain (Peng et al., 2021b).
F&R (LUH)	***Close-range:*** 1D drivability model to generate hammer force (Deeks and Randolph, 1993), FE model for the sound field (Fricke and Rolfes, 2015) ***Long-range:*** PE model (Collins, 1993)	– Axisymmetric model. – Close-range module includes elasticity of the seabed. – 3D effects in terms of varying bathymetry can be included within the all-fluid model approximation in the long-range module.

3 PHYSICS OF THE GENERATED WAVE FIELDS IN IMPACT AND VIBRATORY PILING

This section presents some key features of the emitted wave field during impact piling. The physics of the emitted wave fields is first discussed for each installation method followed by an energy flux analysis in the case of impact piling alone.

In Figure 2, the radiated waves at the exterior to the pile region generated during a single impact of the hammer are shown for radial distances up to 160m for a typical case of the installation of a large size pile (Tsouvalas, 2020). The velocity norm in the soil and fluid media is shown, i.e., $v(r,z,t) = \sqrt{v_r^2(r,z,t) + v_z^2(r,z,t)}$. In the soil, both compressional and shear wave fronts are radiated in the form of Mach cones. The angles of the cones depend on the ratio of the velocities between the waves in the pile and the correspondent waves in the soil region. In addition, solid-fluid interface waves (Scholte waves) are visible at later moments in time, which propagate along the fluid-solid interface.

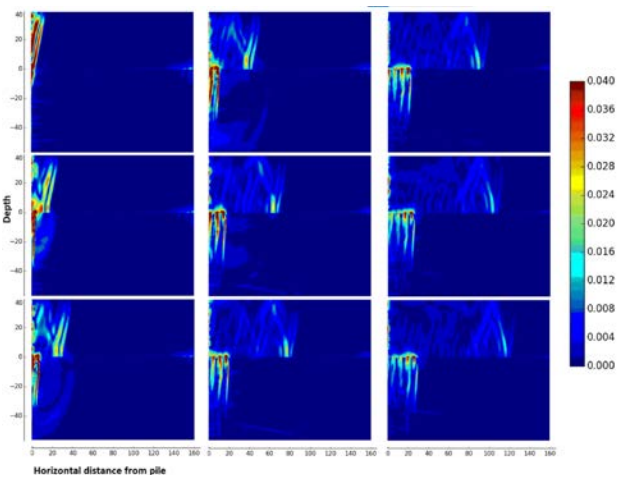

Fig. 2. Pressures in the fluid (z≤25) and velocity norm in the soil (z>25) for several moments in time after the hammer impact. From left to right, the time moments are given in 10−3s: t=6; 12; 16; 24; 30; 45; 72; 96; 120. Simulation results borrowed from [31].

The field in the seawater region consists of pressure waves that span the entire depth of the seawater column (*primary noise path*). These waves are generated by the oscillation of the surface of the shell as the wave train propagates downwards of the pile. Moreover, the excited Scholte waves, which propagate along the seabed surface, induce low-frequency pressure fluctuations in the water column close to the seabed level (*secondary noise path*). These low-frequency waves are clearly distinguished from the initial pressure cones, since they penetrate only slightly into the water zone and propagate at very low speeds. Due to their localized nature, they disturb a finite part of the water column at the vicinity of the seabed-water interface, and hence, their presence is noticeable only within a distance of a few wavelengths from the seabed level. In (Ruhnau et al., 2016), their presence is verified by measurements of geophones positioned on the seabed. Although the horizontal range of influence of the interface waves is generally unknown, since it strongly depends on the contrast of the material properties between the seawater and the upper soil layer, their presence needs to be accounted for when the focus is placed on the design of noise mitigation equipment or when the marine ecosystem is considered particularly rich close to the seabed, i.e., demersal and benthic zones of the water-seabed column. To the best of the authors' knowledge, the effect of the Scholte waves generated by marine piling is very often overlooked in practice.

The radiated wave field in the soil and in the seawater as a result of vibratory pile installation is shown in Figure 3. Results correspond to the case study presented in (Tsouvalas and Metrikine, 2016). Clearly, the wave pattern is different from the one presented previously in the installation with an impact hammer. The coherent Mach cones which could be easily noticed in impact pile driving are not any more visible in this case because the energy enters the water columns from all vertical angles due to the different temporal structure of the excitation. Moreover, the amplitude of the frequency spectrum of the radiated noise varies considerably between impact and vibratory pile driving.

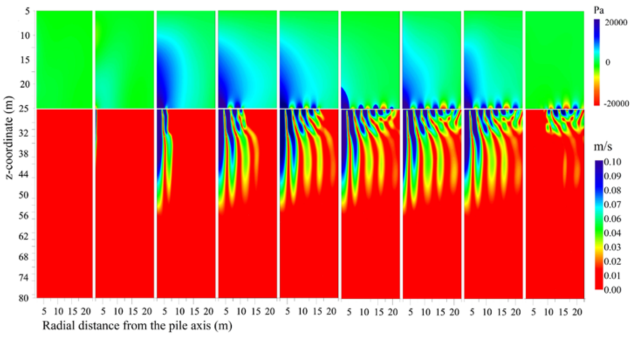

Fig. 3. Pressures in the fluid (z≤25; top part of the figure) and velocity norm in the soil (z>25; bottom part of the figure) for several moments in time after the hammer impact. From left to right, the time moments are given in seconds: t=0.01; 0.07; 0.10; 0.15; 0.20; 0.25; 0.30; 0.50; 0.60.

Figure 4 shows predictions of the SEL and the $L_{p,pk}$ as a function of the horizontal distance from the pile using the model in (Tsouvalas et al., 2019). We first note that the model predictions are within the uncertainty of the measuring equipment given the hydrophones' sensitivity at both locations in which noise measurements were available. Most models described earlier are nowadays capable of reproducing measurements with similar accuracy as illustrated in (Lippert et al., 2018). The $L_{p,pk}$ shows larger variation with distance which can be explained by the fact that it is more sensitive to constructive and destructive interference of the acoustic waves in the seawater. In contrast, the SEL, being an integral quantity representing an energy level, shows a much smoother evolution with range, especially at distances larger than 500 m.

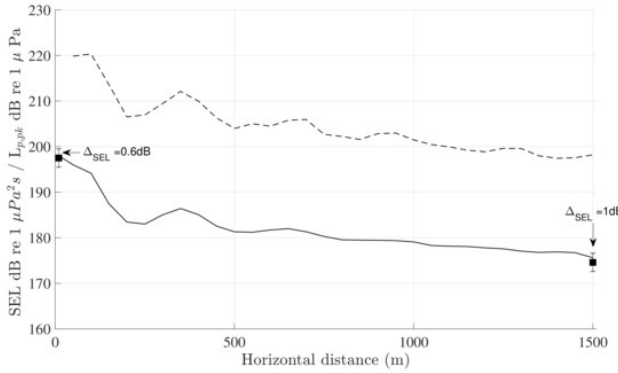

Fig. 4. Evolution of SEL and $L_{p,pk}$ with distance from the pile for the case study analysed in (Tsouvalas, 2020). The dashed line shows the model predictions for the $L_{p,pk}$ and the solid line the predictions for the SEL. Measurement data are also depicted at r=10 m and r=1500 m together with the measurement error bar ±2 dB. Δ_{SEL} denotes the difference between predictions and measurements at the given locations.

Next to the sound levels, it is instructive to examine the radiated wave field under the prism of the energy flux. An energy flux analysis can be of importance for a number of reasons. First, it contributes to the understanding of the energy transfer through seabed and seawater together its evolution with increasing distance from the pile. Second, it allows one to explain possible inefficiencies of the noise mitigation strategies. Third, it gives the possibility to make solid choices on the optimal noise mitigation strategy tailored to the needs of each specific case in terms of the type of mitigation system, the distance from the pile and the deployment strategy.

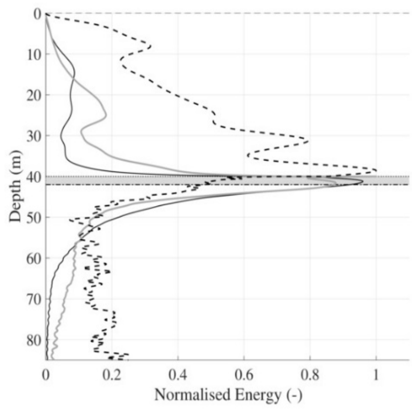

Fig. 5. Energy flux at various distances from the pile as predicted for the BARD Offshore I wind farm case study (Tsouvalas, 2020). Thin black line: r=20 m; thick grey line: r=60 m; thick dashed line: r=140m. The light grey shaded area marks the thickness of the loose marine sediment layer.

Figure 5 shows the normalized (to the maximum per location value) energy fluxes calculated by means of the formulae given in (Tsouvalas and Metrikine, 2014) at various distances for the BARD Offshore I wind farm case (Tsouvalas, 2020). We note that at close distances to the pile the energy is largely concentrated close to the seabed–water interface due to the presence of high-amplitude Scholte waves. The amplitude of the latter diminishes with distance; at 140 m the largest part of the energy is carried by the bulk waves in the seawater. In the same lines, one could examine the flux of energy from the seabed to the water to establish the optimum position for the deployment of a noise mitigation system.

The acoustic energy of the waves can be calculated as a sum of potential energy (related to the pressure) and the kinetic energy related to particle motion. The motion of these particles (represents the mean density of medium) can be quantified as the particle displacement (equivalently particle velocity or particle acceleration), and is an essential metric for assessing the impact of the sound specifically for the fish and invertebrates since their hearing mechanism uses particle motion (Popper and Hawkins,2018; Nedelec et al.,2016). Thus, the calculation and measurement of the particle motion components are significant to provide insight into the impact of offshore pile driving on marine life during the installation. Most advanced models nowadays (Peng et al., 2021) do compute the particle motion in the water column and seabed surface and therefore can be used for such impact assessment studies.

4 NOISE MITIGATION STRATEGIES

Next to the developments in noise prediction modelling, studies on noise mitigation have also been conducted (Koschinski and Lüdemann, 2013). There are in principle two ways to reduce the noise levels caused by pile installation (Verfuß, 2014). The first one is the alteration of the noise source mechanism, i.e., the adoption of a different pile driving procedure such that noise emission is reduced at the source. In this respect, one can either modify the force exerted by the impact hammer or switch to alternative pile driving methods that avoid the generation of high-amplitude shock waves in the pile, e.g., traditional vibratory piling, BLUE Piling or Gentle Driving of Piles (Metrikine et al., 2020). The second way to reduce the noise is to create a so-called anti-noise barrier around the pile. The noise barriers can be categorized into three primary groups on the basis of the underlying noise reduction principle: (i) air bubble curtains in various configurations (Würsig et al., 2000); (ii) casings that enclose the pile in the form of either a depressurized double-walled cylindrical shell (Jansen et al., 2012) or lightweight inflatable fabrics which build an air-column around the pile and resonator-based noise mitigation systems which can take the form of either a fishing net of encapsulated bubbles and foam elements (Bruns et al., 2014) or Helmholtz-type resonators (Elzinga et al., 2019).

4.1 Air Bubble Curtains

The most widely adopted method to mitigate underwater noise is the development of a noise barrier in the seawater column that consists of rising air bubbles. The air bubble cloud is placed around the pile at a given distance in the form of a bubble curtain (Würsig et al., 2000), which is formed by freely rising bubbles created by compressed air injected through series of perforated pipes positioned on the seabed surface (Figure 7). The compressed air is supplied by an air compressor usually positioned on the installation vessel. The impedance contrast between the seawater and the air bubble curtain is significant due to the large differences in density and compressibility of the two media.

Over the last decade, several models have been developed for the predicting the performance of an air-bubble curtain system. A semi-analytical model was developed by Tsouvalas and Metrikine (Tsouvalas and Metrikine, 2016), in which the dynamic interaction between the pile, water, soil and air bubble curtain is captured through a mode-matching technique. The acoustic properties of the bubble curtain are determined by an effective wavenumber theory (Commander and Prosperetti, 1989) assuming the bubbly layer is a homogeneous medium with mono-sized bubble distribution. A model incorporating the hydrodynamic behaviour of bubble breakup and coalescence is developed by Bohne et al. (2019). The various bubble generation and development phases are captured and the acoustic characteristics are deter-mined with a depth- and frequency-dependent transfer function. The FE module including the pile, water, soil and bubble layer described by the bubble dynamic model is used for the noise source generation and propagation. Subsequently, the bubble size distribution is optimized by the two fractions of bubbles, namely large and small bubbles in (Bohne et al., 2020). A semi-analytical model is developed by Peng et al. (2021b), in which the hydrodynamic model by Bohne et al. (2019, 2020) is coupled to the vibroacoustic model for noise prediction from pile driving through a boundary integral formulation. The results indicate that the accurate description of the acoustic characteristics of the bubbly layer is critical for modelling noise mitigation using the DBBC system.

Fig. 7. (Left) Air-bubble cloud released by a perforated pile positioned on the seabed. (Right) Double Big Bubble Curtain (DBBC) deployed around the Giant7 floating piling vessel in the Wikinger OWF, Germany. Source: © Hydrotechnik Lübeck GmbH (https://www.hydrotechnik-luebeck.de/blog/portfolio-item/0003-borkumwest2-00/).

However, solely given the total air injection rate for the bubble curtain, the flow velocity at the nozzle cannot be determined accurately without the examination of the air transportation within the main hose. In a more recent model, a complete modelling approach is proposed including modelling the transport of compressed air from the air-supplied vessel to the hose. The model consists of four modules: (i) a hydraulic model for modelling the transport of com-pressed air from the offshore vessel to the perforated hose located into the sea bed; (ii) a hydrodynamic model for capturing the characteristics of bubble clouds in varying development phases through depth and range; (iii) an acoustic model for predicting the sound insertion loss of the air-bubble curtain; and (iv) a vibroacoustic model for the prediction of underwater noise from pile driving which is coupled to the acoustic model in (iii) through a boundary integral formulation. The flow of the modelling activity is shown in Figure 9. The complete model can be used for the optimization of the DBBC system including the pneumatic system and the deployment of DBBC.

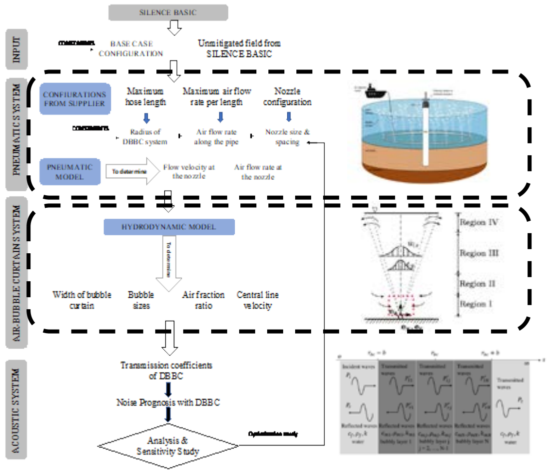

Fig. 9. The activity plot of the multi-physics model for modelling noise mitigation with the use of the air-bubble.

4.2 Pile Casings

Besides the noise mitigation techniques in the receiver locations, the noise can be mitigated at the sound source. Various technologies have been developed and applied at the pile location as pile casing to reduce the generated noise levels at the close distances to the pile. Some of these techniques described below.

4.2.1 Noise mitigation screens (NMS)

The Noise Mitigation Screen (NMS) consists of a double-walled cylindrical shell made of steel placed around the pile at a distance of a few meters from the pile surface. The gap between the inner and the outer wall of the NMS is filled with air (Tsouvalas, 2020). The system can be combined with an air bubble curtain that fills the inter-space between the pile and the inner wall of the NMS, yielding a combined LBC-NMS system (Jansen et al.,2012). Subsequent phases of the installation of a monopile with the NMS at the German offshore wind farm Riffgat are shown in Figure 10.

Fig. 10. The installation of a 6.5 m pile with the use of a Noise Mitigation Screen (IHC Offshore Systems) at the German offshore wind farm Riffgat in the North Sea. In the left and middle pictures, the NMS is positioned by the crane around the monopile. In the right picture, the hydraulic hammer is positioned at the head of the pile and the NMS is invisible Source: Author's personal archive from the Riffgat Offshore Wind Farm (2012).

4.2.2 Lightweight inflatable fabrics

HydroNAS uses a lightweight inflatable fabric, which is restrained internally, to build a continuous column of air surrounding the pile from the seabed to the surface. Upon the inflation of the fabric, a fixed volume panel of air is created which maintains a specified geometry underwater. The cells are modular, stackable and can be configured to fit any water depth and pile size. The system is at its early stage of development and has not yet been tested in full-scale offshore environments.

4.3 Resonator-type Systems

Resonators consist of an array of resonating units that are deployed around the pile to absorb the emitted sound. Resonator-type systems work as acoustic energy sinks, causing internal mechanical vibrations of the latter (Peng et al.,2018). There are several options to design such a device, two of which are described below.

4.3.1 Hydro-Sound-Dampers (HSD)

HSD use nets of air-filled balloons and special PE-foam elements with high dissipative characteristics to reduce noise levels caused by impact piling. HSD rely on multiple mechanisms to reduce the underwater noise: (i) resonant effects of the air-filled balloons and the PE-foam elements fixed in the fishing net. The HSD-elements are adjustable both in terms of diameter and positioning on the net; (ii) dissipation and material damping effects according to the chosen materials and the injected pressure in the air balloons; and (iii) reflection of the sound waves at the interface between the water and the fishing net caused by the impedance mismatch (although this mechanism is less efficient in this case compared to the case of a dense air bubble curtain). The efficacy of the HSD in reducing the noise levels depends on the frequency and volume ratio of the HSD-elements in the net, with ratios of about 1–2% to be sufficient to obtain acceptable noise reduction (Elmer and Savery, 2014). A typical installation set-up with the use of HSD is shown in Figure 11.

Fig. 11. (Left) The HSD system with a length of 40 m hanging from the crane. Source: https://www.offnoise-solutions.com/the-hydro-sound-dampersystem-hsd-system/. (Right) The newly developed AdBm-NAS system showing the resonators in the array (https://adbmtech.com/wp/) (Tsouvalas, 2020).

4.3.2 Helmholtz Resonators (AdBm-NAS)

The AdBm-NAS consists of standard size panels with submersible air-filled Helmholtz resonators that encircle the pile during construction. The steel framework holding the system needs to be designed and fabricated by another contractor. The AdBm system completed successfully a full-scale tests in 2018 (Elzinga et al.,2019).

4.4 Overview of Mitigation Techniques and Spectral Insertion Loss

Table 2 summarizes the most widely used noise mitigation systems, indicating their broadband noise reduction in SEL. It should be noted that the detailed comparison between different noise mitigation systems can be only done under the same installation settings and environmental conditions (Tsouvalas, 2020).

Table 2. Overview of the most widely used noise mitigation systems, and their broadband noise reduction levels. Installed pile data reflect experience gathered until mid-2018 (adapted from (Tsouvalas, 2020)).

Mitigation system	**Number of piles**	**ΔSEL**
Big Bubble Curtain	>1000	~13 for the single BBC and ~17 for the double BBC
Noise Mitigation Screen	>400	~12 without the BBC and ~17 with the BBC
Hydro-Sound Dampers	>250	~15

5 FUTURE CHALLENGES

The state-of-the-art in predictive modelling of sound due to impact piling includes a detailed description of the pile interacting (linearly) with soil and water. Other elements, such as the anvil positioned at the pile head and the hydraulic hammer, are usually disregarded in the acoustic models and are substituted by a force applied at the top of the pile. Such a force can be estimated on the basis of a so-called drivability model (Tsetas et al., 2021). Despite the simplifications above, these models have been proven capable of reproducing measurements with satisfactory accuracy in the case of impact piling (Peng et al., 2021a, Lippert et al., 2018). Future research is focused on the following points: (i) Advanced modelling of the seabed, either by introducing a modified elastic continuum description with frequency-dependent wave speed and attenuation (Buckingham, 2005) or by adopting the theory of poro-elasticity by Biot (Biot, 1962); (ii) Probabilistic modelling in which the uncertainties in the characterisation of the geometry or the properties of the acousto-elastic region are propagated at larger distances from the pile (Lippert and von Estorff, 2014; Caumo et al., 2022); (iii) Pile driving noise predictions in range- and/or angular-dependent environments; (iv) Non-symmetric hammer force (Tsouvalas and Metrikine, 2013; Deng et al., 2016) or inclined piles (Wilkes and Gavrilov, 2017) yielding an azimuthally dependent acoustic field; (v) Simultaneous pile progression into the soil with noise prediction in the near-field. (vi) Challenges associated with the modelling of the various noise mitigation systems and demonstration of the efficacy of those systems for piles of larger diameters and deeper waters (>45 m); (vii) modelling wave emission in the case of vibratory pile driving with the new techniques; and (viii) Modelling and measuring the particle motion during the pile driving operations could help with noise impact assessments specifically for the fish and invertebrates in the test site. A discussion as to most points above is given in (Tsouvalas, 2020). Hereafter, we discuss briefly topics (ii) and (v).

5.1 Propagation of Uncertainties

Most studies on pile driving acoustics are based on deterministic analyses. Such a modelling approach is by far not systematic in spotting the key parameters contributing to uncertainty nor can it be used in a generic framework of uncertainty quantification. Given the large uncertainty in many modelling parameters, especially when it comes to the pile–soil interaction and the characterisation of the seabed, a probabilistic approach that would accommodate a large number of (fast) simulations is largely missing.

A first attempt to follow a probabilistic framework in noise prediction by impact piling is reported by Lippert and von Estorff (2014). However, in that study, the seabed was described by an acoustic model and a (computationally heavy) Monte Carlo approach was chosen for capturing the uncertainty in the seabed properties.

A follow up study, in which uncertainties in seabed characterisation are quantified and propagated to the target distance was recently reported by Caumo, et al., (2022). Due to the high spatial variation in the marine environments, there are many uncertainties in the characterization of the soil parameters both in terms of wave speeds and attenuation of the various waveforms. Such parameters, however, are essential input for an accurate prognosis of the emitted sound field and the seabed vibrations. To deal with uncertainties in the input parameters, probabilistic and statistical approaches have recently been employed as means of quantifying the uncertainty in noise predictions. By employing fast computational models in offshore pile driving (Peng et al., 2021a), the noise distributions can be obtained to define the probability of exceeding a certain sound level. Another objective is to identify correlations between specific soil features and resulted sound levels.

Based on the number of soil strata, it is possible to group the recordings in regions which show similar trends. An analysis of a case study presented by Caumo et al. (2022) is discussed hereafter. The analysis of the soil stratification is done by grouping data that show similar mean and minimum standard deviation. The analysis of variance (ANOVA) is used in this analysis to evaluate sets of data groups for soil layers. Once the layers have been defined, a practical framework is used to determine the optimal parameters for the different distributions (Maximum Likelihood Estimator). The Copula model, based on the rank methods, is then used to investigate the dependence between several random variables. The main advantage provided by this approach is the selection of an appropriate model for the dependence between data sets. The sound level probability density functions can be derived based on various distributions. An example of the results of such a simulation is given in Figure 12 in which the probability of exceedance of a certain sound level can easily be read for a specific case (Caumo et al., 2022).

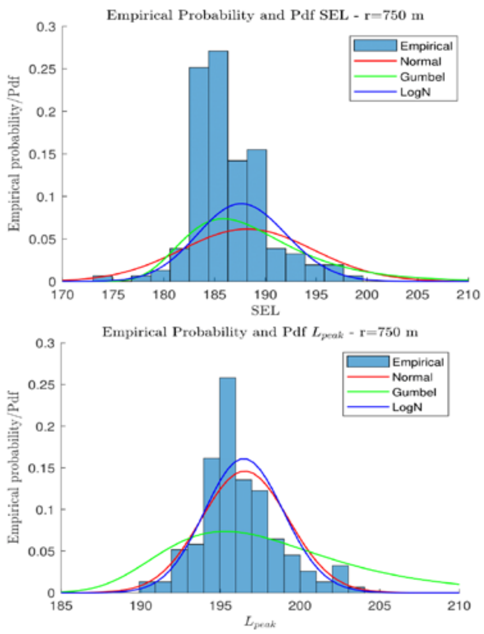

Fig. 12. Probability density distributions (PFDs) of SEL and $L_{p,pk}$ from the uncertainty analysis (in the seabed properties).

5.2 Pile Progression and Noise Prediction

The nonlinear frictional dynamics that take place at the pile-soil interface are complex and not well understood. Some work in this respect trying to identify the frictional losses at the pile–soil interface during piling has been carried out by Fritsch (2008). To date, all existing vibroacoustic models overlook the pile-soil slip and assume that full contact between the pile and the soil is preserved at all times. A few models do consider frictional losses locally at the pile–soil interface (Tsouvalas and Metrikine, 2013; Heitmann et al., 2015] but not the true nonlinear pile-slip dynamics. Thus, all existing models silently hypothesise that by excluding the pile slip in the prediction of noise the error is marginal. Likely, in the case of impact piling, noise measurements seem to confirm the validity of this hypothesis.

In contrast, one should be cautious in generalising this observation to other forms of pile installation in which the progression of the pile into the soil is more smooth. A possible case in which pile progression may be key to accurately capture noise prediction is when vibratory devices are used to install the foundations piles. In contrast to impact piling, which generates a shock wave travelling down the pile inducing local slip at the position of the wave front, in vibropiling standing waves are generated and the pile is gradually pushed into the soil. Thus, the mechanism of pile driving is considerably different as well as the sound field generated.

The effect of pile-slip on noise emission is until now neglected. However, it is important to realised that a perfect pile-soil contact does not only overestimate the energy radiated into shear waves in the soil, but also affects the pile dynamics when a force is exerted at the pile head. To investigate the importance of the pile-soil slip, a realistic case is generated for a pile of 60m length and 5m diameter which is driven 30m into the soil ata region with a bathymetry of 22m. A vibratory force is applied at the pile head, the frequency spectrum of which is given in Figure 13.

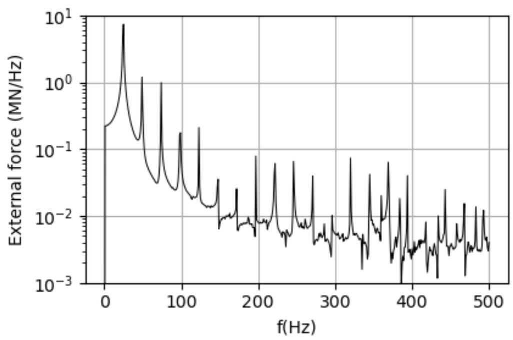

Fig. 13. Frequency spectrum of the vibratory force exerted at the pile head. The force consists of the main driving frequency of 25Hz and several super-harmonics.

Table 3. Status of national and regional noise regulations.

Existing national regulations	Existing regional regulations	Regulations in development or considered
Australia Belgium Brazil Canada Denmark Germany Ireland Mexico New Zealand Taiwan The Netherlands United Kingdom USA Vietnam	ACCOMBAMS ASCOBANS CBD CCAMLR European Union HELCOM IMO IWC NATO OSPAR	Chile China Saudi Arabia Qatar

To evaluate the effect of the boundary condition, the case of perfect contact (no pile-soil slip) is compared with the other (extreme) limit case of zero friction resistance, i.e. a fully sliding surface. Figure 14 compares the near field pressure levels in both cases. It shows that the pile-soil interface condition assumed strongly affects the sound pressure levels, especially at the low end of the frequency spectrum. These frequencies contain most energy in vibratory pile driving. The results presented here imply that the usually applied condition of full contact between pile and soil can yield inaccurate predictions. When the excitation spectrum is broadband, i.e. impact piling, the overall error can be mitigated due to the fact that the overestimation of the levels at certain frequency bands is compensated by the underestimation in some others. This yields overall a reasonable estimation of the noise metrics. However, when the excitation is narrowband, i.e. vibratory pile installation, the error in the prediction of the noise levels can become larger since a systematic under- or overestimation of the levels is possible. Clearly, this is an item worth investigating in the future in light of the new pile driving technologies.

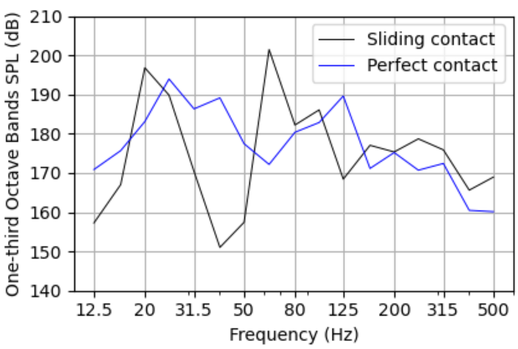

Fig. 14. One-third octave band SPL at r = 10m and 2 m above the seabed for the case of a perfect pile-soil contact (blue line) and idealised sliding pile-soil contact (black line).

6 NOISE REGULATIONS

To understand the adverse effects of the underwater noise, the collaboration between various disciplines (i.e. physicists, biologists, offshore engineers, governmental organizations) are required. As an outcome of this multidisciplinary effort, noise regulations have been introduced for the national and regional noise regulations and mitigation guidelines (Lucke, 2013). The continuous and impulsive properties of sound sources need to be considered when the implementation of these noise criteria and guidelines. For instance, the frequency weighting for the different hearing groups or the duration of the exposure can lead to different species-specific thresholds for TTS, PTS or behavioural disturbance. Southall (2007) and Southall et al. (2019) review existing scientific information and propose criteria for the noise thresholds and auditory frequency weighting functions. Lucke (2020) summarizes the existing underwater noise regulations worldwide, as shown in Table 3.

The authorities can also have different goals and strategies, such as assessing or limiting the noise levels to protect species, requirements of soft-start procedures or deterrent devices to avoid potential impacts. A summary of the various legislations is given in Table 4 below.

Table 4. Summary of sound thresholds in various countries.

Country	Sound thresholds
Germany	Max. unweighted $SEL_{ss,5\%}$ ($L_{E,5\%}$) at 750 m = 160 dB re 1 μPa^{2}s Max. $L_{p,\mathrm{pk}}$ at 750 m = 190 dB re 1 μPa
The Netherlands	Max. unweighted SEL_{ss} ($L_{E,\max}$) at 750 m = 159-172 dB re 1 μPa^{2}s, depending on season and number of piles. After 2023: Max. unweighted SEL_{ss} ($L_{E,\max}$) at 750 m = 168 dB re 1 μPa^{2}s
Belgium	Max. $L_{p,\mathrm{pk}}$ at 750 m = 185 dB re 1 μPa
USA	Max. frequency weighted SEL_{cum} exposure per species group (NMFS, 2018)
UK	England, Wales, and Scotland have different non-prescriptive regulations. The use of the specific protocols is recommended (JNCC, NE and DAERA guidelines, 2020).
Denmark	Max. unweighted SEL_{cum} for fleeing animals = 190 dB re 1 μPa^{2}s

In the United States, various laws and regulations have been applied regarding impacts on individual marine species rather than more general impacts to habitat quality and thus, usually project-based guidelines are applied for the noise impact on specific protected species. The sound maps, including the mitigation measures, provided insight into the noise characteristics with various metrics and their impact on the specific marine animals. Marine Mammal Protection Act [MMPA] and Endangered Species Act [ESA] provide the legislative background in US waters for various activities, including seismic surveys, sonars, pile-driving and explosions, etc. The National Marine Fisheries Service (NMFS) follows the descriptions, categorizes frequency weighing functions and thresholds from Southall et al. (2007) and published revised PTS and TTS criteria in 2018 to assess the noise impact from the impulsive and non-impulsive sound sources (Southall et al., 2019). The impulsive sound sources include seismic surveys, explosions and impact pile driving. In some studies, the non-impulsive or continuous sound sources include ships and vibratory pile driving (Guan and Brookens, 2021). Behavioural disturbances are expected when sound levels exceed 160 dB re 1 µPa (SPL) and continuous sounds exceed 120 dB re 1 µPa (SPL).

In the European Union, EU Marine Strategy Framework Directive requires EU member states to achieve or maintain Good Environmental Status (GES) by 2020. Specifically, GES Descriptor 11 requires underwater noise to be "at levels that do not adversely affect the marine environment". Technical subgroup on underwater noise advice SEL threshold (140 dB re 1 $\mu Pa^2 s$, at the animal) for the behavioural disturbance due to the impulsive sounds (Dekeling et al., 2014). However, the regulations and thresholds can vary among the member nations. In Germany, Federal Maritime and Hydrographic Agency (BSH) applied the first noise rule based on TTS in 2008. One of the key species in German waters is the harbour porpoise. The noise regulations are mainly based on this marine mammal species. In 2013, a standard for the investigation of offshore wind turbines on the marine environment was published (BSH, 2013). According to the German noise monitoring and mitigation measures, the noise characteristics at 750 m should be demonstrated per pulse and should be less than 160 dB re 1 mPa^2 s for SEL and 190 dB re 1 µPa for peak sound pressure level. The noise prognosis and Acoustic Deterrence Devices (ADDs) are required.

In the Netherlands, noise regulations are organized by the Ministry of Infrastructure and Water Management based on the Legislative background of the Nature Conservation Act. The key species are harbour porpoises. Framework for Assessing Ecological and Cumulative Effects (Heinis et al., 2015 & 2019) describes an approach including sound propagation, disturbance area, number of disturbed harbour porpoises, disturbance days, and population-level effects. This framework helps to set the noise limits for offshore wind farm development in the Dutch waters. The noise threshold in this site decisions (Kavelbesluiten) depends on the season and the number of piles. However, the framework suggests a single SEL threshold to be used as 168 dB re 1 μPa^2 s at 750 m after 2023. Deterring the marine animals (e.g., using ADDs) from the vicinity of the pile prior to the start of the piling is required to avoid the risk of PTS in harbour porpoises. The framework is regularly updated, so this threshold value may change in the future.

Each country in the United Kingdom has its own legislation, which is non-prescriptive and activity-centric. The UK regulations advise using the acoustic deterrent devices before the pile-driving activities and soft start procedure during the first 20 minutes of the pile driving. Five harbour porpoise Special Areas of Conservation (SACs) were introduced in 2019. In these areas, no significant disturbance is allowed to maintain the Favourable Conservation Status (FCS) for harbour porpoises. New noise regulations, which are habitat- and species-centric, is under revision.

7 OVERVIEW

In this paper, an overview is presented on the developments in the field of pile driving noise and vibrations. The review includes the modelling works in noise and vibration prognosis when piles are installed offshore, the available noise mitigation techniques, and the developments in the noise regulatory framework. Future challenges are highlighted and some of those are discussed in more detail. This review could serve as a basis for the further development of models and regulations in the field of underwater noise from offshore pile installation.

REFERENCES

1) Ainslie, M.A. Standard for Measurement and Monitoring of Underwater Noise, Part I. Physical Quantities and Their Units; Report No. TNO-DV 2011 C235; Nederlandse Organisatie voor Toegepast-Natuurwetenschappelijk Onderzoek (TNO): Den Haag, The Netherlands, 2011.
2) Bailey, H.; Senior, B.; Simmons, D.; Rusin, J.; Picken, G.; Thompson, P.M. Assessing underwater noise levels during pile-driving at an offshore windfarm and its potential effects on marine mammals. Mar. Pollution Bull. 2010, 60, 888–897.
3) Biot, M.A. Mechanics of Deformation and Acoustic Propagation in Porous Media. J. Appl. Phys. 1962, 33, 1482–1498.
4) Bohne, T.; Grießmann, T.; Rolfes, R. (2019): Modeling the noise mitigation of a bubble curtain, The Journal of the Acoustical Society of America, 146:2212.
5) Bohne, T.; Grießmann, T.; Rolfes, R. (2020): Development of an efficient buoyant jet integral model of a bubble plume coupled with a population dynamics model for bubble breakup and coalescence to predict the transmission loss of a bubble curtain, International Journal of Multiphase Flow, 132.
6) Brandt, M.J.; Höschle, C.; Diederichs, A.; Betke, K.; Matuschek, R.; Nehls, G. Seal scarers as a tool to deter harbour porpoises from offshore construction sites. Mar. Ecol. Prog. Ser. 2013, 475, 291–302.
7) Bruns, B.; Kuhn, C.; Stein, P.; Gattermann, J.; Elmer, K.H. The new noise mitigation system 'Hydro Sound Dampers': History

of development with several hydro sound and vibration measurements. In Proceedings of the Inter-Noise 2014 Conference in Australia, Melbourne, Australia, 16–19 November 2014; pp. 1–9.

8) BSH,(2013): Standard Investigation of the Impacts of Offshore Wind Turbines on the Marine Environment (StUK 4),(https://www.bsh.de/DE/PUBLIKATIONEN/_Anlagen/Downloads/Offshore/Standards/Standard-Investigation-impacts-offshore-wind-turbines-marine-environment_en.html), Last accessed 25/02/2022
9) Buckingham, M.J. Compressional and shear wave properties of marine sediments: Comparisons between theory and data. J. Acoust. Soc. Am. 2005, 117, 137–152.
10) Caumo, G. Probabilistic framework for the soil modelling in the sound propagation during impact pile driving. MSc thesis TU Delft (2022).
11) Collins, M.D. A split-step Padé solution for the parabolic equation method. J. Acoust. Soc. Am. 1993, 93, 1736–1742.
12) Commander, K.W.; Prosperetti, A (1989): Linear pressure waves in bubbly liquids: Comparison between theory and experiments, The Journal of the Acoustical Society of America, 85, 732–746.
13) Dähne, M.; Tougaard, J.; Carstensen, J.; Rose, A.; Nabe-Nielsen, J. Bubble curtains attenuate noise from offshore wind farm construction and reduce temporary habitat loss for harbour porpoises. Mar. Ecol. Prog. Ser. 2017, 580, 221–237.
14) De Jong, C.A.F.; Ainslie, M.A.; Blacquière, G. Standard for Measurement and Monitoring of Underwater Noise, Part II: Procedures for Measuring Underwater Noise in Connection with Offshore wind Farm Licensing; Report No. TNO-DV 2011 C251; Nederlandse Organisatie voor Toegepast-Natuurwetenschappelijk Onderzoek (TNO): Den Haag, The Netherlands, 2011.
15) Deeks, A.J.; Randolph, M.F. Analytical modelling of hammer impact for pile driving. Int. J. Numer. Anal. Methods Geomech. 1993, 17, 279–302.
16) Dekeling, R.P.A., Tasker, M.L., Graaf, A.J. van der, Ainslie, M.A., Andersson, M.H., André, M., Borsani, J.F., Brensing, K., Castellote, M., Cronin, D., Dalen, J., Folegot, T., Leaper, R., Pajala, J., Redman, P., Robinson, S.P., Sigray, P., Sutton, G.,Thomsen, F., Werner, S., Wittekind, D. & Young, J.V., (2014): Monitoring Guidance for Underwater Noise in European Seas, Part III: Background Information and Annexes, JRC Scientific and Policy Report EUR 26556 EN, Publications Office of the European Union, Luxembourg. doi: 10.2788/2808.
17) Deng, Q.; Jiang, W.; Tan, M.; Xing, J.T. Modeling of offshore pile driving noise using a semi-analytical variational formulation. Appl. Acoust. 2016, 104, 85–100.
18) Dolman, S.; Simmonds, M. Towards best environmental practice for cetacean conservation in developing Scotland's marine renewable energy. Mar. Policy 2010, 34, 1021–1027.
19) Elzinga, J.; Mesu, A.; van Eekelen, E.; Wochner, M.; Jansen, E.; Nijhof, M. Installing Offshore Wind Turbine Foundations Quieter: A Performance Overview of the First Full-Scale Demonstration of the AdBm Underwater Noise Abatement System. In Proceedings of the Offshore Technology Conference, Houston, TX, USA, 6–9 May 2019.
20) Erbe, C. International regulation of underwater noise. Acoust. Aust. 2013, 41, 12–19.
21) ESA, https://www.fisheries.noaa.gov/topic/laws-policies#endangered-species-act, , Last accessed on 25/02/2022, Last accessed on 25/02/2022.
22) European Wind Energy Association (EWEA). Offshore Wind in Europe—Key Trends and Statistics 2018; Technical Report; WindEurope asbl/vzw: Brussels, Belgium, 2019.
23) Farcas, A.; Thompson, P.M.; Merchant, N.D. Underwater noise modelling for environmental impact assessment. Environ. Impact Assess. Rev. 2016, 57, 114–122.
24) Finneran, J.J. Noise-induced hearing loss in marine mammals: A review of temporary threshold shift studies from 1996 to 2015. J. Acoust. Soc. Am. 2015, 138, 1702–1726.
25) Fricke, M.B.; Rolfes, R. Towards a complete physically based forecast model for underwater noise related to impact pile driving. J. Acoust. Soc. Am. 2015, 137, 1564–1575.
26) Fried, L.; Shukla, S.; Sawyer, S. Chapter 26—Growth Trends and the Future of Wind Energy. In Wind Energy Engineering; Letcher, T.M., Ed.; Academic Press: Cambridge, MA, USA, 2017; pp. 559–586.
27) Fritsch, M. Zur Modellbildung der Wellenausbreitung in Dynamisch Belasteten Pfählen (about the Modelling of Wave Propagation in Dynamically Loaded Piles). Ph.D. Thesis, Technische Universität Braunschweig, Braunschweig, Germany, 2008.
28) Graham, I.M.; Pirotta, E.; Merchant, N.D.; Farcas, A.; Barton, T.R.; Cheney, B.; Hastie, G.D.; Thompson, P.M. Responses of bottlenose dolphins and harbor porpoises to impact and vibration piling noise during harbor construction. Ecosphere 2017, 8, e01793.
29) Guan, S.; Brookens, T., Vignola, J., (2021): Use of Underwater Acoustics in Marine Conservation and Policy: Previous Advances, Current Status, and Future Needs. J. Mar. Sci. Eng., 9, 173.
30) Hastie, G.; Merchant, N.D.; Götz, T.; Russell, D.J.F.; Thompson, P.; Janik, V.M. Effects of impulsive noise on marine mammals: Investigating range-dependent risk. Ecol. Appl. 2019, 29, e01906.
31) Heinis, F., de Jong, C.A.F. von Benda-Beckmann, S. Binnerts B., (2019): Framework for Assessing Ecological and Cumulative Effects – 2018. Cumulative effects of offshore wind farm construction on harbour porpoises. TNO.
32) Heinis, F., de Jong, C.A.F., Werkgroep Onderwatergeluid, (2015): Cumulatieve effecten van impulsief onderwatergeluid op zeezoogdieren. TNO-rapport TNO R10335. TNO, Den Haag.
33) Heitmann, K.; Mallapur, S.; Lippert, T.; Ruhnau, M.; Lippert, S.; von Estorff, O. Numerical determination of equivalent damping parameters for a finite element model to predict the underwater noise due to offshore pile driving. Euronoise 2015, 2020, 605–610.
34) Herbert-Read, J.E.; Kremer, L.; Bruintjes, R.; Radford, A.N.; Ioannou, C.C. Anthropogenic noise pollution from pile-driving disrupts the structure and dynamics of fish shoals. Proc. R. Soc. B Biol. Sci. 2017, 284, 20171627.
35) Jansen, H.W.; De Jong, C.A.; Jung, B.C. Experimental assessment of the insertion loss of an underwater noise mitigation screen for marine pile driving. In Proceedings of

the 11th European Conference on Underwater Acoustics 2012 (ECUA 2012), Edinburgh, UK, 2–6 July 2012.
36) Kastelein, R.A.; Hoek, L.; Gransier, R.; de Jong, C.A.F. Hearing thresholds of a harbor porpoise (Phocoena phocoena) for playbacks of multiple pile driving strike sounds. J. Acoust. Soc. Am. 2013, 134, 2302–2306.
37) Koschinski, S.; Lüdemann, K. Development of Noise Mitigation Measures in Offshore Wind Farm Construction 2013; Technical Report; Federal Agency for Nature Conservation (Bundesamt für Naturschutz), BfN: Bonn, Germany, 2013.
38) Lippert, S.; Nijhof, M.; Lippert, T.; Wilkes, D.; Gavrilov, A.; Heitmann, K.; Ruhnau, M.; von Estorff, O.; Schafke, A.; Schafer, I.; et al. COMPILE—A Generic Benchmark Case for Predictions of Marine Pile-Driving Noise. IEEE J. Ocean. Eng. 2016, 41, 1061–1071.
39) Lippert, S.; Von Estorff, O.; Nijhof, M.J.; Lippert, T. COMPILE II—A benchmark of pile driving noise models against offshore measurements. In Proceedings of the INTER-NOISE 2018—47th International Congress and Exposition on Noise Control Engineering: Impact of Noise Control Engineering, Chicago, IL, USA, 26–29 August 2018.CHAPTER 4
40) Lippert, T.; Ainslie, M.A.; von Estorff, O. Pile driving acoustics made simple: Damped cylindrical spreading model. J. Acoust. Soc. Am. 2018, 143, 310–317.
41) Lippert, T.; Galindo-Romero, M.; Gavrilov, A.N.; von Estorff, O. Empirical estimation of peak pressure level from sound exposure level. Part II: Offshore impact pile driving noise. J. Acoust. Soc. Am. 2015, 138, EL287–EL292.
42) Lippert, T.; von Estorff, O. The significance of parameter uncertainties for the prediction of offshore pile driving noise. J. Acoust. Soc. Am. 2014, 136, 2463–2471.
43) Lozano-Minguez, E.; Kolios, A.; Brennan, F. Multi-criteria assessment of offshore wind turbine support structures. Renew. Energy 2011, 36, 2831–2837.
44) Lucke K., (2020): DOSIT presentation handouts, https://dosits.org/wp-content/uploads/2020/11/DOSITS-Regulatory-Approaches-to-Underwater-Noise_Klaus-Lucke_public.pdf, Last accessed on 25/02/2022
45) Lucke, K., Siemensma, M. ,(2013): International regulations on the impact of pile driving noise on marine mammals - A literature review. (Rapport / IMARES Wageningen UR; No. C044/13). IMARES. https://edepot.wur.nl/306911
46) Lucke, K.; Siebert, U.; Lepper, P.A.; Blanchet, M.A. Temporary shift in masked hearing thresholds in a harbor porpoise (Phocoena phocoena) after exposure to seismic airgun stimuli. J. Acoust. Soc. Am. 2009, 125, 4060–4070.
47) MacGillivray, A.O. Finite difference computational modeling of marine impact pile driving. In Proceedings of the 2015 Euronoise Conference, Maastrcht, The Netherlands, 1–3 June 2015; Volume 136, pp. 623–628.
48) Martin, S.B.; Barclay, D.R. Determining the dependence of marine pile driving sound levels on strike energy, pile penetration, and propagation effects using a linear mixed model based on damped cylindrical spreading. J. Acoust. Soc. Am. 2019, 146, 109–121.
49) Mercer, J. Colossus Revisited: A Review and Extension of the Marsh-Schulkin Shallow Water Transmission Loss Model (1962); Defense Technical Information Center: Fort Belvoir, VA, USA, 1985.
50) Metrikine, A.V.; Tsouvalas, A.; Segeren, M.L.; Elkadi, A.S.; Tehrani, F.S.; Gómez, S.S.; Atkinson, R.; Pisanó, F.; Kementzetzidis, E.; Tsetas, A.; et al. GDP: A new technology for Gentle Driving of (mono)Piles. In Proceedings of the 4th International Symposium on Frontiers in Offshore Geotechnics, Austin, TX, USA, 16–19 August 2020.
51) MMPA,https://www.fws.gov/international/laws-treaties-agreements/us-conservation-laws/marine-mammal-protection-act.html , Last accessed on 25/02/2022
52) National Marine Fisheries Service (NMFS), (2016): Technical Guidance for Assessing the Effects of Anthropogenic Sound on Marine Mammal Hearing: Underwater Acoustic Thresholds for Onset of Permanent and Temporary Threshold Shifts. U.S. Dept. of Commer., NOAA. NOAA Technical Memorandum NMFS-OPR-55, 178 p.
53) National Marine Fisheries Service (NMFS), (2018):Revisions to: Technical Guidance for Assessing the Effects of Anthropogenic Sound on Marine Mammal Hearing (Version 2.0): Underwater Thresholds for Onset of Permanent and Temporary Threshold Shifts. U.S. Dept. of Commer., NOAA. NOAA Technical Memorandum NMFS-OPR-59
54) Nedelec, S.L., Campbell, J., Radford, A.N., Simpson, S.D. and Merchant, N.D. (2016), Particle motion: the missing link in underwater acoustic ecology. Methods Ecol Evol, 7: 836-842.
55) Oh, K.Y.; Nam, W.; Ryu, M.S.; Kim, J.Y.; Epureanu, B.I. A review of foundations of offshore wind energy convertors: Current status and future perspectives. Renew. Sustain. Energy Rev. 2018, 88, 16–36.
56) PACSYS: FEA/BEM Solutions. Available online: http://www.pafec.info/pafec/ (accessed on 11 June 2020).
57) Park, J.; Seong, W.; Lee, K. Modeling of underwater noise from pile driving using coupled finite element and parabolic equation model with improved parabolic equation starting field. J. Acoust. Soc. Am. 2013, 134, 4114.
58) Peng, Y.; Tsouvalas, A.; Metrikine, A.; Belderbos, E., (2018): Modelling and development of a resonator-based noise mitigation system for offshore pile driving. In Proceedings of the 25th International Congress on Sound and Vibration 2018 (ICSV 2018): Hiroshima Calling, Hiroshima, Japan, 8–12 July 2018; Volume 8; pp. 5070–5077.
59) Peng, Y.; Tsouvalas, A.; Stampoultzoglou, T.; Metrikine, A (2021a): A fast computational model for near- and far-field noise prediction due to offshore pile driving, The Journal of the Acoustical Society of America, 149(3):1772–1790.
60) Peng, Y.; Tsouvalas, A.; Stampoultzoglou, T.; Metrikine, A. (2021b): Study of the Sound Escape with the Use of an Air Bubble Curtain in Offshore Pile Driving. J. Mar. Sci. Eng., 9, 232.
61) Perveen, R.; Kishor, N.; Mohanty, S.R. Off-shore wind farm development: Present status and challenges. Renew. Sustain. Energy Rev. 2014, 29, 780–792.
62) Popper A.N., Hawkins A.D., 2018, The importance of particle motion to fishes and invertebrates, The Journal of the Acoustical Society of America 143, 470.
63) Popper, A.; Hastings, M. The effects of anthropogenic sources of sound on fishes. J. Fish Biol. 2009, 75, 455–489.

64) Ruhnau, M.; Heitmann, K.; Lippert, T.; Lippert, S.; Von Estorff, O. Understanding soil transmission paths of offshore pile driving noise - Seismic waves and their implications. In Proceedings of the INTER-NOISE 2016—45th International Congress and Exposition on Noise Control Engineering: Towards a Quieter Future, Hamburg, Germany, 21–24 August 2016.
65) Sertlek, H.O.; Ainslie, M.A. A depth-dependent formula for shallow water propagation. J. Acoust. Soc. Am. 2014, 136, 573–582.
66) Sertlek, H.O.; Ainslie, M.A.; Heaney, K.D. Analytical and Numerical Propagation Loss Predictions for Gradually Range-Dependent Isospeed Waveguides. IEEE J. Ocean. Eng. 2019, 44, 1240–1252.
67) Southall, B.L., Bowles, A.E., Ellison, W.T., Finneran, J.J., Gentry, R.L., Greene, C.R., Jr. Kastak, D., Ketten, D.R., Miller, J.H., Nachtigall, P.E., Richardson, W.J., Thomas, J.A., & Tyack, P.L., (2007): Marine mammal noise exposure criteria: Initial scientific recommendations. Aquatic Mammals 33: 411–521.
68) Southall, B.L., Finneran, J.J., Reichmuth, C., Nachtigall, P.E., Ketten, D.R., Bowles, A.E., Ellison, W.T., Nowacek, D.P. & Tyack P.L., (2019): Marine Mammal Noise Exposure Criteria: Updated Scientific Recommendations for Residual Hearing Effects. Aquatic Mammals 45(2): 125-232, DOI 10.1578/AM.45.2.2019.125
69) Stöber, U.; Thomsen, F. Effect of impact pile driving noise on marine mammals: A comparison of different noise exposure criteria. J. Acoust. Soc. Am. 2019, 145, 3252–3259.
70) Thomsen, K.E. Chapter Eleven—Commonly Used Installation Methods. In Offshore Wind; Thomsen, K.E., Ed.; Elsevier: Boston, MA, USA, 2012; pp. 157–184.
71) Tsetas, A.; Tsouvalas, A.; Metrikine, A.V. Installation of Large-Diameter Monopiles: Introducing Wave Dispersion and Non-Local Soil Reaction. *J. Mar. Sci. Eng.* 2021, *9*, 313.
72) Tsouvalas, A. Underwater Noise Emission Due to Offshore Pile Installation: A Review. *Energies* 2020, *13*, 3037.
73) Tsouvalas, A. Underwater Noise Generated by Offshore Pile Driving. Ph.D. Thesis, Delft University of Technology, Delft, The Netherlands, 2015.
74) Tsouvalas, A., Metrikine, A. V. (2014): A three-dimensional vibroacoustic model for the prediction of underwater noise from offshore pile driving, Journal of Sound and Vibration, 333(8) 2283- 2311.
75) Tsouvalas, A., Metrikine, A. V. (2016): Noise reduction by the application of an air-bubble curtain in off-shore pile driving, Journal of Sound and Vibration, 371 150-170.
76) Tsouvalas, A.; Metrikine, A. Structure-Borne Wave Radiation by Impact and Vibratory Piling in Offshore Installations: From Sound Prediction to Auditory Damage. J. Mar. Sci. Eng. 2016, 4, 44.
77) Tsouvalas, A.; Metrikine, A.V. A semi-analytical model for the prediction of underwater noise from offshore pile driving. J. Sound Vib. 2013, 332, 3232–3257.
78) Tsouvalas, A.; Peng, Y.; Metrikine, A. Underwater Noise Generated By Offshore Pile Driving: A Pile-Soil-Water Vibroacoustic Model Based On A Mode Matching Method. In Proceedings of the 5th Underwater Acoustics Conference and Exhibition 2019 (UACE2019), Hersonissos, Greece, 30 June–5 July 2019; pp. 667–674.
79) Verfuß, T. Noise mitigation systems and low-noise installation technologies. In Ecological Research at the Offshore Windfarm alpha ventus; Springer: Wiesbaden, Germany, 2014; pp. 181–191.
80) Von Pein, J.; Klages, E.; Lippert, S.; von Estorff, O. A hybrid model for the 3D computation of pile driving noise. In Proceedings of the OCEANS 2019—Marseille, Marseille, France, 17–20 June 2019; pp. 1–6.
81) Warrington, D. Theory and Development of Vibratory Pile-Driving Equipment. In Proceedings of the Offshore Technology Conference, Houston, TX, USA, 1–4 May 1989.
82) Westwood, E.K.; Tindle, C.T.; Chapman, N.R. A normal mode model for acousto-elastic ocean environments. J. Acoust. Soc. Am. 1996, 100, 3631–3645.
83) Wilkes, D.R.; Gavrilov, A.N. Sound radiation from impact-driven raked piles. J. Acoust. Soc. Am. 2017, 142, 1–11.
84) Wood, M.A. Modelling and Prediction of Acoustic Disturbances from Off-Shore Piling. Ph.D. Thesis, University of Southampton, Southampton, UK, 2016.
85) Wu, X.; Hu, Y.; Li, Y.; Yang, J.; Duan, L.; Wang, T.; Adcock, T.; Jiang, Z.; Gao, Z.; Lin, Z.; et al. Foundations of offshore wind turbines: A review. Renew. Sustain. Energy Rev. 2019, 104, 379–393.
86) Würsig, B.; Greene, C.R., Jr.; Jefferson, T. Development of an air bubble curtain to reduce underwater noise of percussive piling. Mar. Environ. Res. 2000, 49, 79–93.
87) Zampolli, M.; Nijhof, M.J.J.; de Jong, C.A.F.; Ainslie, M.A.; Jansen, E.H.W.; Quesson, B.A.J. Validation of finite element computations for the quantitative prediction of underwater noise from impact pile driving. J. Acoust. Soc. Am. 2013, 133, 72–81.